Stoch Environ Res Risk Assess
DOI 10.1007/s00477-008-0269-8

ORIGINAL PAPER

Nonlinearity and complexity in gravel bed dynamics

Arvind Singh · Stefano Lanzoni · Efi Foufoula-Georgiou

Abstract The dynamics of river bed evolution are known to be notoriously complex affected by near-bed turbulence, the collective motion of clusters of particles of different sizes, and the formation of bedforms and other large-scale features. In this paper, we present the results of a study aiming to quantify the inherent nonlinearity and complexity in gravel bed dynamics. The data analyzed are bed elevation fluctuations collected via submersible sonar transducers at 0.1 Hz frequency in two different settings of low and high discharge in a controlled laboratory experiment. We employed surrogate series analysis and the transportation distance metric in the phase-space to test for nonlinearity and the finite size Lyapunov exponent (FSLE) methodology to test for complexity. Our analysis documents linearity and underlying dynamics similar to that of deterministic diffusion for bed elevations at low discharge conditions. These dynamics transit to a pronounced nonlinearity and more complexity for high discharge, akin to that of a multiplicative cascading process used to characterize fully developed turbulence. Knowing the degree of nonlinearity and complexity in the temporal dynamics of bed elevation fluctuations can provide insight into model formulation and also into the feedbacks between near-bed turbulence, sediment transport and bedform development.

Keywords Nonlinearity · Complexity · Bedforms · Finite size Lyapunov exponent (FSLE) · Diffusion

A. Singh (✉) · E. Foufoula-Georgiou
St. Anthony Falls Laboratory and National Center for Earth-Surface Dynamics, Department of Civil Engineering, University of Minnesota, 2 Third Avenue SE, Minneapolis, MN, USA
e-mail: sing0336@umn.edu

E. Foufoula-Georgiou
e-mail: efi@umn.edu

S. Lanzoni
Dipartimento di Ingegneria Idraulica, Marittima, Ambientale e Geotecnica, and International Center for Hydrology ''Dino Tonini'', Università di Padova, Padua, Italy
e-mail: lanzo@idra.unipd.it

1 Introduction

The evolution of alluvial river beds is the result of a number of often strongly nonlinear processes which give rise to the extraordinary large variety of patterns observed in nature. In gravel bed rivers, where the dominant form of sediment transport is bedload, both field observations (Drake et al. 1988) and laboratory experiments (Kirkbride 1993; Nelson et al. 1995) suggest that most of the transport occurs by the collective motion of clusters of particles mobilized by turbulent sweep events and outward interactions, while a relatively smaller contribution is associated with bursts (see also review of Best 1993). Clearly, the bed evolution is likely to be strongly affected by the intermittent process whereby coherent turbulent structures are randomly generated, grow and decay in the near-wall region.

Coherent structure dynamics, in turn, depend on the range of scales characterizing a given bed topography, and the flow variability at a given point contains both locally derived flow structures and structures inherited from upstream (Hardy et al. 2007). The bed evolution is further complicated by the formation of either free bedforms (e.g., Gomez et al. 1989), arising as a result of the instability of a cohesionless bed subject to a turbulent flow, or bedforms forced by geometrical constraints (e.g., channel curvature) (Seminara 1998). Finally, the heterogeneous character of the sediment leads to patterns associated with a spatial and

temporal rearrangement of the grain size distribution of the sediments (Parker 1991) which are strongly related to the different mobility of particles having different diameter (Wilcock and McArdell 1993, 1997).

It then clearly appears that river bed evolution, even in the simplest case of a flat bed configuration, is an extremely complex phenomenon whose understanding needs the use of refined theoretical, experimental and data analysis techniques.

Several contributions have been so far devoted to the study of the spatial properties of water-worked gravel bed surfaces measured both in the laboratory and in the field (e.g., see Nikora and Walsh 2004, and references therein). In addition to conventional statistical parameters (i.e., standard deviation, skewness and kurtosis) of the bed elevation spatial distribution, second-order and higher-order structure functions have been proved particularly helpful for exploring the statistical properties and potential multiscaling behavior of bed elevations fields (Aberle and Nikora 2006). In a recent study, the multiscale statistical structure of the temporal evolution of bed elevation fluctuations at several locations on the evolving gravel bed under steady-state conditions has also been analyzed and the presence of a multiscaling behavior has been reported (Singh et al. 2008).

In the present contribution, a different type of analysis of temporal elevation series is performed aiming at quantifying the nonlinearity and complexity in gravel bed dynamics. It is noted that these dynamics are internally generated by the system itself rather than by an external stochastic forcing, since the discharge is kept constant and the system is under steady state conditions. To the best of our knowledge, the only other study that attempted a similar analysis is that of Gomez and Phillips (1999) who analyzed sediment transport rates (interestingly collected from a controlled laboratory experiment conducted in the same flume almost 20 years ago; see Hubbell et al. 1987). The overall goal of that study was to identify deterministic sources of uncertainty, or unexplained variation, in the time series of bedload transport rates by computing how much of the observed variability (quantified in terms of Kolmogorov entropy) was not explained by bedform migration effects. The assumption was made that the variability (entropy) due to bed migration would be fully captured by a Hamamori probability distribution. It is noted that the Hamamori distribution is derived from sediment movement over a purely geometrical self-similar bed morphology (Hamamori 1962) and does not account for the natural variability in bedform shapes and sizes. It is also restricted to sediment transport rates that are at most four times the mean rate—not the case in most observed series including the series analyzed in Gomez and Phillips (1999).

The purpose of the present study is to revisit the problem of quantifying the deterministic complexity in gravel bed dynamics with an assumption-free methodology and using more powerful techniques recently developed in the study of nonlinear systems (e.g., Aurell et al. 1997). The adopted methodologies have been proven to give a deep insight in other complex geophysical processes such as fluid turbulence (Aurell et al. 1996a; Boffetta et al. 2002), atmospheric boundary layer dynamics (Basu et al. 2002) and dispersive mixing in porous media (Kleinfelter et al. 2005), among others.

The paper is organized as follows. In Sect. 2 we briefly describe the bed elevation data collected in two laboratory experiments under low and high discharge conditions. Section 3 introduces the mathematical methodology used first to identify the presence or absence of inherent nonlinearity in time series and second the finite size Lyapunov exponent (FSLE) methodology to quantify the complexity and predictability of processes exhibiting many scales of motion. In Sect. 4, results of the analysis of the temporal sequences of bed elevation data series are presented. Finally, Sect. 5 presents concluding remarks and suggestions for future research.

2 Experimental data

The data examined in the present contribution were collected during a series of experiments conducted in the Main Channel facility at the St. Anthony Falls Laboratory, University of Minnesota. The channel is 2.74-m wide and has a maximum depth of 1.8 m. It is a partial-recirculating flume in that it has the ability to recirculate the sediment while the water flows through the flume without recirculation. Water for the channel was drawn directly from the Mississippi River, with a maximum discharge capacity of 8,000 l/s. The channel has a 55-m long test section and, in the experiments reported here, a poorly sorted gravel bed extended over the last 20 m of this test section. The gravel used in these experiments had a broad particle size distribution characterized by $d_{50} = 11.3$ mm, $d_{16} = 4.27$ mm and $d_{84} = 23.07$ mm. More details on this experimental setting can be found in Singh et al. (2008).

Measurements of bed elevation and sediment transport were taken at a range of discharges corresponding to different bed shear stresses. Here we focus our attention on the series of bed elevations collected under two different discharges: a low discharge case, with a discharge of 4,300 l/s, corresponding to a dimensionless bed stress of about twice the critical value (Shields stress = 0.085 using median diameter) and a high discharge, 5,500 l/s, corresponding to a Shields stress about five times the critical value (Shields stress = 0.196). For both bed stress

conditions, the flume was allowed to run long enough prior to data collection such that a dynamic equilibrium was achieved in transport and slope adjustment of the water surface and bed. Determination of the dynamic equilibrium state was made by checking that the 60-min average sediment flux was stabilized to an almost constant value during the flume run. The bed elevation was then recorded over a span of approximately 20 h for each experiment, by using submersible sonar transducers, with a frequency of 0.1 Hz and a vertical precision of ~ 1 mm. Figure 1 displays the time series of bed elevations measured at a location aligned with the main channel axis for both the low (Fig. 1a) and the high (Fig. 1c) discharge conditions over a period of 10 h during which the bed-elevation and sediment flux series were stationary. The low bed stress run (Fig. 1a) produced a nearly plane channel bed, with only limited topographic variations, i.e. without obvious large scale structures in the bed elevation (the standard deviation in the bed is 10.06 mm, compared to the initial d_{50} grain size of 11.3 mm). On the contrary, the higher stress run (Fig. 1c) generated substantial bed variability at large scale in the form of dunes, with intermediate to particle-scale fluctuations superimposed on these larger-scale features. In this study we focus on comparing these two runs in terms of the complexity of the underlying forming processes imprinted in the time series of bed elevation fluctuations. The analysis methodologies we employed are briefly described below.

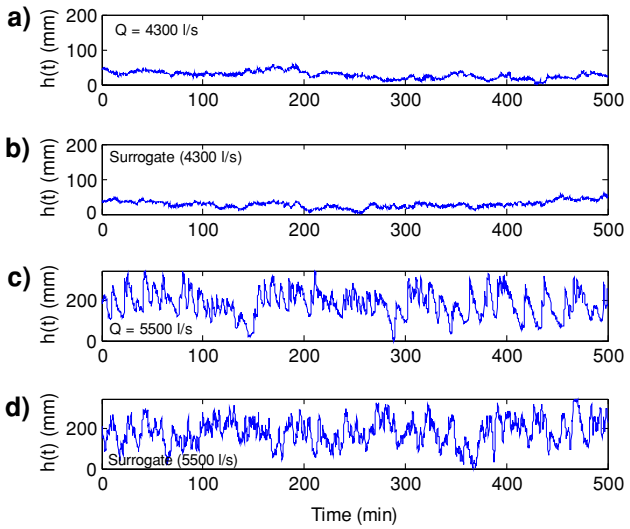

Fig. 1 Bed elevation time series for **a** low discharge (4,300 l/s; bed elevation mean is 27.38 mm and standard deviation 10.06 mm) and **c** high discharge (5,500 l/s; bed elevation mean is 185.51 mm and standard deviation 66.61 mm). Surrogate series for **b** low and **d** high discharge. Notice that although it is difficult to distinguish any difference between the original and the surrogate series, the surrogate series in high discharge has linear underlying dynamics while the original series is shown to be highly nonlinear (see Fig. 2)

3 Analysis methodologies

3.1 Test for nonlinearity

Nonlinearity is a necessary condition for deterministic chaos and thus methodologies for testing whether a time series has been generated by a linear or inherently nonlinear process have gained considerable attention in the literature. By inherent nonlinear process it is meant a process whose nonlinearity is not external, i.e., the result of a static nonlinear transformation applied on an otherwise linear underlying process, but it is weaved into its dynamics such as for example in a series arising as a result of a multiplicative cascade generator, a popular phenomenological model for turbulence (e.g., Frisch 1995). Detection of nonlinearity is not a trivial task and several methods are available, as for example based on "reversibility", information-theoretic approaches, singular value decomposition, and the use of "surrogates" (e.g., see a review in Basu and Foufoula-Georgiou 2002 and references therein). Here we adopt a surrogate-based methodology. Surrogate series maintain the probability density function (pdf) and correlation structure (and thus spectrum) of the original series but destroy any inherent nonlinearity since the process of generating the surrogates randomizes the phases in the Fourier space.

The method we used for surrogate series generation is the iterative amplitude adjusted Fourier transform (IAAFT) method of Schreiber and Schmitz (1996). This method is an improvement of the earlier amplitude adjusted Fourier transform (AAFT) method of Theiler et al. (1992), and iteratively adjusts both the pdf and linear correlation structure to minimize their deviation from the original series. The reader is referred to the original publications for details to supplement the brief exposition presented below.

The surrogate series $\{s_n\}$ is assumed to be generated by a process of the form

$$s_n = S(y_n), \quad y_n = \sum_{i=1}^{M} a_i y_{n-1} + \sum_{i=1}^{N} b_i \eta_{n-1}, \tag{1}$$

where S could be any invertible nonlinear function, $\{y_n\}$ is the underlying linear process, $\{a_n\}$ and $\{b_n\}$ are constants, and $\{\eta_n\}$ is Gaussian white noise. The steps involved in the generation of surrogate series are as follows:

1. Randomly shuffle the data points of the original series $\{x_n^o\}$ to destroy any correlation or nonlinear relationship, while keeping the pdf unchanged. The reshuffled series is the starting point for the iteration $\left\{s_n^{(o)}\right\}$.
2. Construct the discrete Fourier transform of the series at the ith iteration $\left\{s_n^{(i)}\right\}$, and adjust the amplitudes to recreate the power spectrum of the original data. Keep the phases unchanged. Perform inverse Fourier transform.

3. The pdf will no longer be correct. Transform the data to the correct pdf by rank ordering and replacing each value with the value in the original series $\{x_n^o\}$ with the same rank. This will result in an updated series $\{s_n^{(i+1)}\}$.
4. Repeat steps 2 and 3 until discrepancy in the power spectrum is below a threshold, or the sequence stops changing (reaches a fixed point). In this manner a surrogate data series can be generated with an identical pdf and optimally similar power spectrum to the original series.

Figure 1b and 1d shows two realizations of the surrogate series corresponding to the bed elevation series for low and high flow discharge. It is noted that in both cases it is difficult to distinguish visually any difference between the original series and their surrogates (compare Fig. 1a to 1b and 1c to 1d. It is reminded that the original and surrogate series share the same pdf and correlation structure or spectrum, but the surrogate series contain only linear correlation). However, as it will be demonstrated later, our methodologies depict important differences in the case of high discharge, emphasizing the presence of inherent nonlinearity in the bed forming process.

Once an ensemble of surrogate series is generated, a probabilistic metric of the "distance" between each one of those series to the original series $\{x_n^o\}$ and between multiple realizations of the surrogate series $\{s_n\} = \{x_n^i\}, i = 1, \ldots, N_s$ is formed. If the original series were linear, these two distance metrics would overlap as one would not be able to discriminate the original series from members of the ensemble of surrogates; however, if they do not overlap, nonlinearity in the original series can be inferred with confidence.

Following Basu and Foufoula-Georgiou (2002), we use the transportation distance functions $d_{oi} = d(x_n^o, x_n^i)$ and $d_{ij} = d(x_n^i, x_n^j), (i \neq j)$ to measure, respectively, the difference in the long term behavior between the original data set and the ith surrogate data set and the mutual distances between surrogates. The idea is to transform two given scalar time series (x, y) in vector time series (X, Y) by phase-space reconstruction using an embedding dimension (e) and an integer delay (τ), thus obtaining an e-dimensional embedding space $\mathcal{R}^e$ which captures the dynamics of the x and y systems' attractors (Moeckel and Murray 1997). The details of determining embedding dimension and delay can be found in Kennel et al. (1992), Hegger et al. (1999). In practice, a box in the reconstructed phase space, $\mathcal{R}^e$, containing both the X and Y vector time series is divided into a finite number B_k, $k = 1,\ldots,b$ of sub boxes, each characterized by the discretized probability measures p_k and q_k defined as

$$p_k = \sum_{l=1}^{b} \mu_{kl}, \quad q_k = \sum_{l=1}^{b} \mu_{kl}, \quad l = 1, \ldots, b \tag{2}$$

where $\mu_{kl} \geq 0$ defines the amount of "material" (information) shipped from box B_k to box B_l. These constraints ensure that the initial and final probability distributions are preserved and allow us to determine the set $M(p, q)$ [with $p = (p_1,\ldots,p_b)$ and $q = (q_1,\ldots,q_b)$] of all transportation plans. The transportation function is then obtained by minimizing (e.g., through the network simplex algorithm) the transportation cost

$$d(p, q) = \inf_{\mu \in M(p,q)} \sum_{k,l=1}^{b} \mu_{kl} \delta_{kl} \tag{3}$$

where δ_{kl} is the taxi cab metric (Moeckel and Murray 1997) normalized to the embedding dimension between the centres of B_k and B_l. If the pdf of the transportation distances d_{oi} between the original series and the surrogates is distinct from the pdf of the mutual distances d_{ij} between the surrogates, nonlinearity is inferred. Details of the methodology and examples of its application to known linear and nonlinear series, e.g., autoregressive series, Lorenz series, stochastic Van der Pol oscillator series, and the Santa Fe Institute competition series, can be found in Basu and Foufoula-Georgiou (2002).

3.2 Quantification of complexity

It is well known that many natural systems, although deterministic, are characterized by a limited degree of predictability owing to the presence of deterministic chaos which makes small errors in the initial conditions to grow exponentially fast with time (e.g., Lorenz 1969). In the traditional sense, predictability is assessed via computation of the maximum Lyapunov exponent which dictates that the predictability time is

$$T_p \approx \frac{1}{\lambda_{max}} \ln \frac{\Delta}{\delta} \tag{4}$$

where λ_{max} is the leading (or maximum) Lyapunov exponent, measuring the average exponential rate of separation of nearby trajectories, δ is the size of the initial (strictly infinitesimal) perturbation, and Δ is the (still small) accepted error tolerance. The above formula holds only for infinitesimal perturbations, and, by construction, it cannot assess the predictability in systems with many scales of variability, such as turbulence which possesses a hierarchy of eddy turnover times. In those multiscale systems the predictability time T_p is determined by the nonlinear mechanism responsible for the error growth and it is not captured by λ_{max} which is governed by the linearized equations of motion, given the assumption of

small perturbations. To address these issues, Aurell et al. (1996b) proposed a generalization of the maximum Lyapunov exponent method. Specifically, they introduced the quantity $T_p(\delta, \Delta)$ which is the time it takes for a finite perturbation to grow from an initial size δ (in general not infinitesimal) to a tolerance level Δ. The so-called finite size Lyapounov exponent (FSLE) $\lambda(\delta, \Delta)$ is then the average of some function of this predictability time, such that if both δ and Δ are infinitesimally small one would recover the usual Lyapunov exponent:

$$\lambda(\delta, \Delta) = \left\langle \frac{1}{T_p(\delta, \Delta)} \right\rangle \ln\left(\frac{\Delta}{\delta}\right). \quad (5)$$

Various methodologies are available for computing finite-size Lyapunov exponent (see Aurell et al. 1997). In the present contribution we have adopted the method of Boffetta et al. (1998).

4 Results and discussion

4.1 Nonlinearity

The results of nonlinearity tests carried out on the two time series of bed elevations are reported in Fig. 2. For low discharge conditions (Fig. 2a), the pdf of the transportation distance between the original series and the surrogates overlaps the one obtained by considering multiple realizations of the surrogates. On the other hand, Fig. 2b shows that for the high discharge case the pdfs of the transportation distance between each surrogate series and the original time series and between multiple realizations of surrogates are completely different, suggesting that strong nonlinearities are inherent in the processes which shaped the bed morphodynamics. These nonlinearities are likely to be connected to the irregular and unsteady large-scale bedforms, mainly dunes, observed in this high flow experiment, promoting the formation of patterns of sorting and leading to a strong reworking of the sediment bed (Klaassen 1990; Blom et al. 2003).

To shed light into the above findings, we proceed with the following analysis guided by some recent findings in Singh et al. (2008). We synthetically generated two series with known underlying dynamics: a fractional Brownian motion (fBm) series and a multiplicative cascade series. The fBm series (with the Hurst exponent $H = 0.5$) is known to have linear underlying dynamics, arising from the integration of white noise. A multiplicative cascade series, on the other hand, arises from a nonlinear (multiplicative) mechanism of energy transfer from larger to smaller scales and thus possesses clearly nonlinear underlying dynamics. These latter dynamics cannot be rendered linear by any external transformation but rather are intrinsically embedded in all scales of variability of the process. In this work, we generated multiplicative cascade series using the random wavelet cascade (RWC) model (e.g., Arneodo et al. 1997) parameterized by two coefficients: c_1 and c_2. These two parameters dictate how the energy breaks down from larger to smaller scales, i.e., they characterize the probability distribution of the multiplicative weights of the cascade generator. Here we set $c_1 = 0.7$ and $c_2 = 0.1$ on the basis of the results recently obtained by Singh et al. (2008). This study employed a wavelet-based multifractal formalism and reported that the spectrum of scaling exponents of the same bed elevation fluctuation series analyzed here is well described by a quadratic model with c_1 and c_2 ranging in the intervals 0.53–0.76 and 0.06–0.14, respectively.

For visual comparison, Fig. 3 shows the fluctuations (computed as first order differences) of the original bed elevation series at low discharge (Fig 3a), the generated fBm series with $H = 0.5$ and the same standard deviation as the original series (Fig. 3b), the original bed elevation series at high discharge (Fig. 3c) and the generated RWC series (Fig. 3d) with $c_1 = 0.7$ and $c_2 = 0.1$ It is noted that there is much more "clustering" in the bed elevation series at high discharge than at low discharge which mathematically is depicted by the larger parameter c_2 (0.1 at high discharge vs. 0 at low discharge). More details of this multifractal analysis and interpretation of the parameters c_1 and c_2 can be found in Singh et al. (2008).

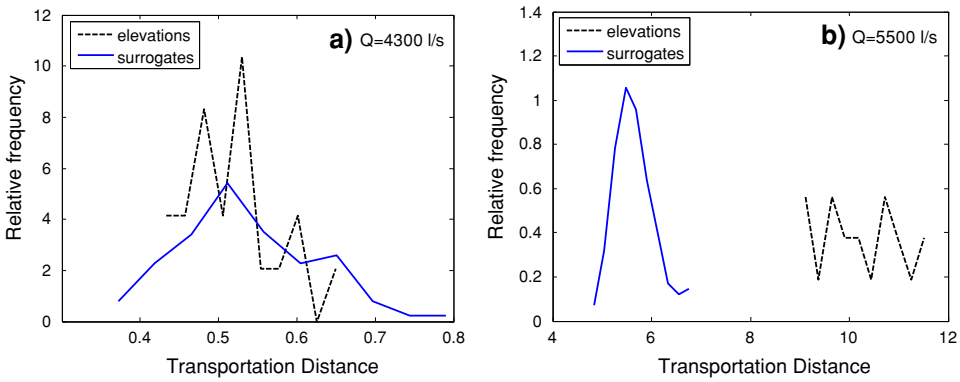

Fig. 2 Probability density function (pdf) of the transportation distances between the original series and the surrogates (*broken lines*), and among the surrogates (*solid lines*) for **a** low discharge, and **b** high discharge runs. Notice the linear underlying dynamics in the case of low discharge (overlapping pdfs) and the nonlinear dynamics in the case of high discharge (distinct pdfs)

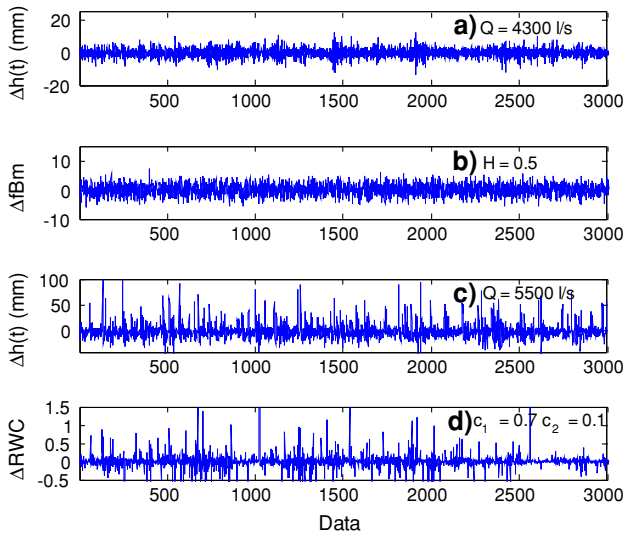

Fig. 3 Fluctuations (first order differences) of **a** measured bed elevation series for low discharge (4,300 l/s), **b** generated fBm series ($H = 0.5$), **c** measured bed elevation series for high discharge (5,500 l/s), and **d** generated random wavelet cascade (RWC) series with parameters $c_1 = 0.7$ and $c_2 = 0.1$

The nonlinearity test described in Sect. 3 was applied to these two generated series. As was expected, the results of the test shown in Fig. 4 correctly depict the inherent linearity of the fBm series and the strong nonlinearity of the RWC series. Comparison of Figs. 2 and 4 gives more confidence to conclude the presence of linear underlying dynamics in gravel bed formation at low discharge conditions which progressively evolve to strongly nonlinear dynamics at high flow conditions (i.e., when the bed shear stress is well above the critical value for incipient motion of sediments). The complexity analysis to follow will shed more light to those conclusions.

4.2 Complexity and predictability

As discussed before, bed elevation fluctuations are known to exhibit multiple scales of variability (e.g., see Nikora and Walsh 2004; Singh et al. 2008) and thus the FSLE approach is a more appropriate methodology for quantifying complexity, than is the standard maximum Lyapunov exponent analysis.

The delay time and embedding dimension adopted in the analysis of the bed elevation series for low and high discharge were chosen to be $d = 10$ and $e = 3$ following the mutual information and false nearest neighbor approaches, respectively (see Kantz and Schreiber 1997), and these algorithms were implemented using the TISEAN package (Hegger et al. 1999). Figure 5a displays the Lyapunov exponent for the two series as a function of the initial perturbation size $\delta = 1$ mm, while Fig. 5b shows the predictability time T_p (in seconds) for the same two series as a function of the prescribed tolerance level Δ ($\Delta = r\delta$, where r is the so-called threshold factor and is assumed to be as $\sqrt{2}$ in this work. (For more details about the threshold factor see Aurell et al. 1997.)

The following observations are worthwhile. First, from Fig. 5b it is observed that the high-discharge bed elevation series is less predictable (more complex) than the series at low-discharge. This is not surprising given the previous results which inferred a pronounced inherent nonlinearity in the high-discharge bed elevation series and simpler linear dynamics for the case of low discharge. It is also interesting to observe that for an initial error of $\delta = 1$ mm (measurement precision) the predictability time associated to a tolerance level of the order of the coarser sediment grain size ($\propto d_{84} = 23.07$ mm) is of the order of 2×10^2 and 4×10^3 seconds for high and low flow condition here examined, an information which can be used to assess the

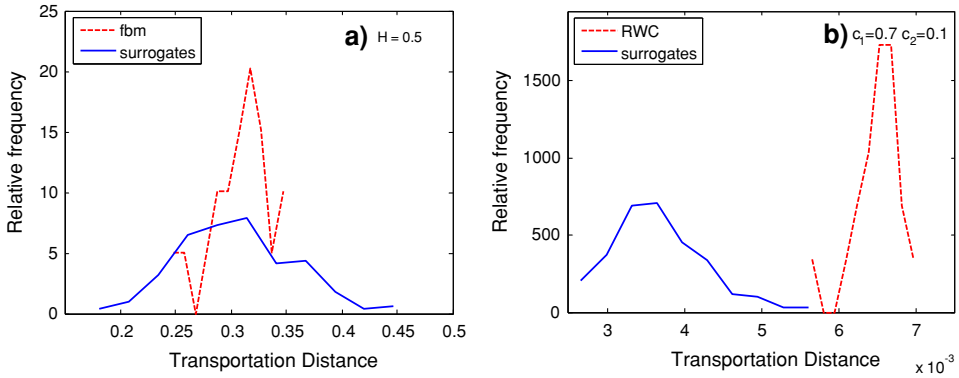

Fig. 4 **a** Probability density function (pdf) of the transportation distances between the synthetically generated fractional Brownian motion series (fBm) with $H = 0.5$ and the surrogates (*broken lines*) and among the surrogates (*solid lines*); **b** same but for synthetically generated random wavelet cascade (RWC) series with $c_1 = 0.7$ and $c_2 = 0.1$. The comparison clearly depicts the expected linearity of the fBm series (overlapping pdfs) and the inherent nonlinearity of the RWC series (distinct pdfs). Notice the similarity with the results of Fig. 2 which displays the same analysis for the original bed elevation series at low and high discharge conditions, respectively

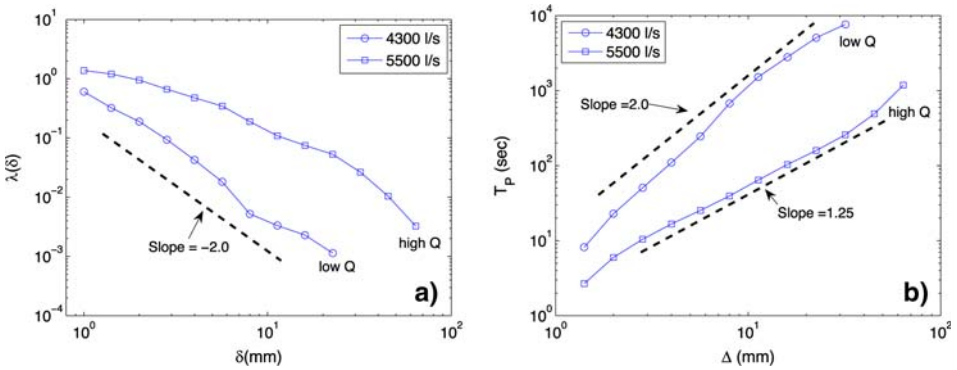

Fig. 5 **a** Finite size Lyapunov exponent (FSLE) $\lambda(\delta)$ as a function of perturbation δ for bed elevation at low discharge (*circle*) and high discharge (*square*). The line of slope -2 (deterministic diffusive behavior) is also shown; **b** Predictability time T_p, based on FSLE, as a function of prediction error tolerance Δ for bed elevation at low discharge (*circle*) and high discharge (*square*). The initial perturbation was specified to be $\delta = 1$ mm

performance of mechanistic models of sediment transport. Second, from Fig. 5a it is interesting to observe that for larger δ, the FSLE has a slope of -2.0, i.e., $\lambda(\delta) \propto \delta^{-2}$, a behavior consistent with that of deterministic diffusion (e.g., Aurell et al. 1997). To verify this assertion, we generated a series of equal length to the bed elevation series, using the 1D Lagrangian map

$$x_{n+1} = x_n + a\sin(2\pi x_n) \tag{6}$$

which is a well-known model for deterministic diffusion, and performed the FSLE on this series. Figure 6 shows the theoretically expected behavior of the size-dependent Lyapunov exponent for this series, that is, $\lambda(\delta) \propto$ const for small values of δ, while $\lambda(\delta) \propto \delta^{-2}$ for larger values of δ. The similarity of this behavior to that of Fig. 5a for the low-discharge bed elevation series is worth noting and calls for further exploration.

It is encouraging that for the low-discharge series the linearity inference (Fig. 2a), the similarity to a fBm with $H = 0.5$ (compare Figs. 3a, 3b and 4a to 2a), and the inference that the complexity of this series is similar to that of deterministic diffusion (compare Figs. 5a, 6), are all consistent with each other. It is also encouraging that for the high-discharge elevation series, the presence of strong nonlinearity (Fig. 2b), similar to that of a multiplicative cascade series (Fig. 4b) and the higher complexity (lower predictability) of this series (Fig. 5b), are consistent to each other and also consistent with the multifractal analysis results of this series in Singh et al. (2008). An interesting result is that the predictability time seems to follow a power law relationship with the tolerance level of prediction in both low and high discharge conditions, that is

$$T_p \sim \Delta^{\beta} \tag{7}$$

where β is approximately 2 for low discharge and 1.25 for high discharge (directly quantifying the lesser degree of

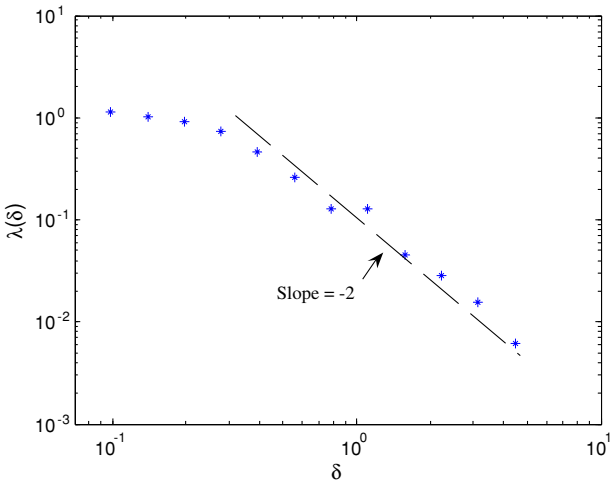

Fig. 6 FSLE for deterministic diffusion generated by the 1D Lagrangian map $x_{n+1} = x_n + a\sin(2\pi x_n)$, with $a = 0.8$, corresponding to a diffusion coefficient $D = 0.18$

predictability of bed elevation series at high discharge). This relationship can be of practical significance (sets the upper limit of prediction) and should also be reproducible by mechanistic models of sediment entrainment and transport.

5 Concluding remarks

The goal of this paper was to gain insight into the complexity of the processes governing the temporal evolution of gravel bed elevation by objectively analyzing data from a controlled experimental setting. Specifically, we analyzed bed elevation series under low and high discharge conditions (i.e., with a bed shear stress slightly higher or significantly higher than the critical value for incipient sediment motion) to quantify the presence of inherent

nonlinearity and the degree of complexity (the higher the complexity the lesser the degree of predictability of the series). We used the phase-space transportation distance metric to quantify the presence of nonlinearity in the series and the finite size Lyapounov exponent (FSLE) methodology to quantify complexity.

Overall, our results indicate that under higher discharge conditions, the presence of bedforms and substantial bed variability at all scales (from grain size to well-formed dunes) leads to bed elevation series whose nonlinearity and complexity are demonstrably more pronounced compared to the bed elevation series under low discharge. For low discharge conditions, in the substantial absence of bedforms, the bed elevation series was found statistically indistinguishable from a series with linear underlying dynamics and also exhibiting a behavior similar to that of deterministic diffusion. Conversely, for high discharge conditions, the temporal evolution of bed elevation was clearly nonlinear and, in fact, it showed a behavior similar to that of a multiplicative cascade process, which is extensively used to model turbulent velocity fluctuations. Given that bedforms are shaped by the near-bed turbulence which is expected to posses nonlinear and multi-scale structure for both low and high discharge, the differences found in the nonlinearity and complexity of bed elevation fluctuations in the two different discharges is interesting and requires further study. They highlight the nontrivial (and mostly unknown) two-way interactions between turbulent flow, sediment transport and bedforms and call for further experiments and analysis under a continuum of discharges and turbulence regimes.

We consider this study as a first step towards a more comprehensive study aimed to: (1) understand the complex multiscale dynamics of bed elevation and the resulting sediment transport series; (2) make inferences about the inherent predictability, or expected upper limit to prediction, by any mechanistic model of sediment transport; and (3) parameterize this complexity in terms of macroscopic flow and sediment properties (e.g., mean bed shear stress, grain size distribution) to provide useful information for physical model development.

Acknowledgments This research was supported by the National Center for Earth-surface Dynamics (NCED), a Science and Technology Center funded by NSF under agreement EAR-0120914. The support by the Joseph T. and Rose S. Ling Professorship in Environmental Engineering at the University of Minnesota is also gratefully acknowledged. A series of experiments (known as StreamLab06) were conducted at the St. Anthony Falls Laboratory as part of an NCED program to examine physical-biological aspects of sediment transport (http://www.nced.umn.edu). Computer resources were provided by the Minnesota Supercomputing Institute, Digital Technology Center at the University of Minnesota. The authors are grateful to David Olsen for his assistance in the preparation of the manuscript.

References

Aberle J, Nikora V (2006) Statistical properties of armored gravel bed surfaces. Water Resour Res 42:W11414. doi:10.1029/2005WR004674

Arneodo A, Muzy JF, Roux SG (1997) Experimental analysis of self-similarity and random cascade processes: application to fully developed turbulence data. J Phys II 7:363–370

Aurell E, Boffetta G, Crisanti A, Paladin G, Vulpiani A (1996a) Growth of noninfinitesimal perturbations in turbulence. Phys Rev Lett 77:1262–1265

Aurell E, Boffetta G, Crisanti A, Paladin G, Vulpiani A (1996b) Predictability in systems with many characteristic times: the case of turbulence. Phys Rev E 53:2337–2349

Aurell E, Boffetta G, Crisanti A, Paladin G, Vulpiani A (1997) Predictability in the large: an extension of the concept of Lyapunov exponent. J Phys A Math Gen 30:1–26

Basu S, Foufoula-Georgiou E (2002) Detection of nonlinearity and chaoticity in time series using the transportation distance function. Phys Lett A 301:413–423

Basu S, Foufoula-Georgiou E, Porté-Agel F (2002) Predictabilty of atmospheric boundary-layer flow as function of scale. Geophys Res Lett 29:2038. doi:10.1029/2002GL015497

Best JL (1993) On the interactions between turbulent flow structure, sediment transport and bedform development: some considerations from recent experimental research. In: Clifford NJ, French JR, Hardisty J (eds) Turbulence: perspectives on flow and sediment transport. Wiley, NY

Blom A, Ribberink JS, de Vriend HJ (2003) Vertical sorting in bed forms: flume experiments with a natural and a trimodal sediment mixture. Water Resour Res 39:1025. doi:10.1029/2001WR001088

Boffetta G, Crisanti A, Paparella F, Provenzale A, Vulpiani A (1998) Slow and fast dynamics in coupled systems: a time series analysis view. Phys D 116:301–312

Boffetta G, Cencini M, Falconi M, Vulpiani A (2002) Predictability: a way to characterize complexity. Phys Rep 356:367–474

Drake TG, Shreve RL, Dietrich WE, Whiting PJ, Leopold LB (1988) Bedload transport of fine gravel observed by motion pictures. J Fluid Mech 192:193–217

Frisch U (1995) Turbulence: the legacy of A.N. Kolmogorov. Cambridge University Press, New York

Gomez B, Phillips JD (1999) Deterministic uncertainty in bed load transport. J Hydraul Eng 125:305–308

Gomez B, Naff RL, Hubbel DW (1989) Temporal variations in bedload transport rates associated with the migration of bedforms. Earth Surf Proc Land 14:135–156

Hamamori A (1962) A theoretical investigation on the fluctuation of bedload transport. Delft Hydraulics Lab. Rep R4. Delft Hydraulics Laboratory, Delft

Hardy RJ, Lane SR, Ferguson RI, Parsons DR (2007) Emergence of coherent flow structures over a gravel surface: a numerical experiment. Water Resour Res 43:W03422. doi:10.1029/2006WR004936

Hegger R, Kantz H, Schreiber T (1999) Practical implementation of nonlinear time series methods: the Tisean package. Chaos 9:413–435

Hubbell DW, HH Stevens, JV Skinner and JP Beverage (1987) Laboratory data on coarse-sediment transport for bedload-sampler calibrations, U.S. Geological Survey Water-Supply Paper 2299. U.S. Geological Survey, Washington DC

Kantz H, Schreiber T (1997) Nonlinear time series analysis. Cambridge University Press, Cambridge

Kennel MB, Brown R, Abarbanel HDI (1992) Determining embedding dimension for phase-space reconstruction using a geometrical construction. Phys Rev A 45:3403–3411

Kirkbride A (1993) Observations of the influence of bed roughness on turbulence structure in depth limited flows over gravel beds. In: Clifford NJ, French JR, Hardisty J (eds) Turbulence: perspectives on flow and sediment transport. Wiley, NY

Klaassen GJ (1990) Sediment transport in armoured rivers during floods-literature survey. Tech. Rep. Q790, Delft Hydraulics, Delft, The Netherlands

Kleinfelter N, Moroni M, Cushman JH (2005) Application of finite-size lyapunov exponent to particle tracking velocitmetry in fluid mechanics experiments. Phys Rev E 72:056306

Lorenz EN (1969) The predictability of a flow which possesses many scales of motion. Tellus 21:289–307

Moeckel R, Murray B (1997) Measuring the distance between time series. Phys D 102:187–194

Nelson JM, Shreve RL, McLean R, Drake TG (1995) Role of near-bed turbulence structure in bed load transport and bed form mechanics. Water Resour Res 31:2071–2086

Nikora V, Walsh J (2004) Water-worked gravel surfaces: high-order structure functions at the particle scale. Water Resour Res 40:W12601. doi:10.1029/2004WR003346

Parker G (1991) Some random notes on grain sorting. In: Proceedings of grain sorting seminar IAHR, pp 20–76

Schreiber T, Schmitz A (1996) Improved surrogate data for nonlinearity tests. Phys Rev Lett 77:635–638

Seminara G (1998) Stability and morphodynamics. Meccanica 33:59–99

Singh A, Fienberg K, Jerolmack DJ, Marr JG, Foufoula-Georgiou E (2008) Experimental evidence for statistical scaling and intermittency in sediment transport rates. J Geophys Res Earth (in press)

Theiler J, Eubank S, Longtin A, Galdrikian B, Farmer JD (1992) Testing for nonlinearity in time series: the method of surrogate data. Phys D 58:77–94

Wilcock PR, McArdell BW (1993) Surface-based fractional transport rates: mobilization thresholds and partial transport of a sand-gravel sediment. Water Resour Res 29:1297–1312

Wilcock PR, McArdell BW (1997) Partial transport of sand/gravel sediment. Water Resour Res 33:235–245